J. Fluid Mech. (1971), *vol.* 45, *part* 2, *pp.* 225–246
Printed in Great Britain

Drag reduction in rough pipes

By P. S. VIRK

Department of Chemical Engineering, Massachusetts Institute of Technology, Cambridge, Massachusetts, U.S.A.

(Received 30 December 1969 and in revised form 3 August 1970)

Drag reduction caused by dilute, distilled water solutions of four polyethyleneoxides and one polyacrylamide, molecular weights respectively $0{\cdot}1 \times 10^6$ to 8×10^6 and 13×10^6, was studied experimentally in one smooth and three sand-roughened pipes, relative roughnesses (R/k) 15, 23, 35, all of about 0·34 in. inside diameter. The onset of drag reduction in the rough pipes occurred at the same wall shear stress as in smooth; the onset wall shear stress was essentially independent of polymer concentration, varied inversely as the square of polymer radius of gyration and was unaffected by the flow régime, hydraulically smooth, transitional or fully rough, during which onset occurred. Following onset a flow régime was observed wherein the fractional slip, i.e. fractional increase in mean velocity relative to solvent at a given friction velocity, obtained with a given polymer solution in a rough pipe was the same as the fractional slip in the smooth pipe despite marked differences in the respective rough and smooth friction factors. This 'effectively smooth' régime prevailed for values of non-dimensional roughness $k^{+*} < k^+ < k_{es}^+$ from onset, k^{+*}, to an upper limit given by $k_{es}^+ \sim 50$ for all of the present experiments. For $k^+ > k_{es}^+$, the fractional slip in the rough pipes was always less than that corresponding to smooth and was a function of relative roughness as well as flow and polymeric parameters. The maximum drag reduction possible in the rough pipes was limited by an asymptote which was independent of polymeric parameters. Under asymptotic conditions, friction factors in all the rough pipes identically obeyed the smooth pipe friction factor relation for $k^+ < 12$; the onset of roughness at $k^+ \sim 12$ indicated that the maximum viscous sublayer thickness attained during drag reduction was approximately $2\frac{1}{2}$ times Newtonian.

1. Introduction

Drag reduction by dilute polymer solutions in turbulent pipe flow (Toms 1948) is by now well known and recent experimental studies (e.g. Savins 1964; Elata, Lehrer & Kahanovitz 1966; Virk *et al.* 1967; Seyer & Metzner 1969) have demarcated many aspects of this phenomenon in smooth pipes. While the physical mechanism responsible for drag reduction remains obscure, the experimental evidence does indicate that the polymer-turbulence interaction most affects the region very close to the pipe wall. Experiments in rough pipes are thus of particular interest because they offer the possibility of inferring features of the wall-flow structure from relatively simple friction factor measurements. The

rough wall case is also of interest in possible practical applications of drag reduction.

Drag reduction in rough pipes has been reported previously (Root 1966; Lindgren & Hoot 1968; McNally 1968; White 1969; Spangler 1969) but the available information is of a very preliminary nature. The results of Root (1966) were probably inadvertent, being contained in a patent concerning the use of polymeric additives in oil well fracturing, an operation which involved such high flow rates that the commercial pipe employed was hydraulically rough. Lindgren & Hoot (1968) first conclusively demonstrated drag reduction in a rough pipe by dilute solutions of a polyethyleneoxide in water but gave only qualitative results. McNally (1968), also using a polyethyleneoxide in water, conducted separate experiments in a smooth and a sand-roughened pipe of nearly the same inside diameters. With increasing flow rate, the drag reduction observed in the rough pipe increased to a maximum, then decreased and almost disappeared; the decrease in drag reduction was attributed to polymer degradation *in situ*. White (1969), employing aqueous solutions of a guar gum and a polyethyleneoxide, found that some polymer solutions which reduced drag significantly in smooth pipes yielded no drag reduction in a pipe with a coarsely threaded inside diameter. Spangler (1969) studied drag reduction with a single solution of an acrylamide-acrylic acid copolymer in three pipes of initially equal inside diameter in which sharp-edged threads of different depth were cut. In the two lesser rough pipes, drag reduction was observed to increase, peak and then decrease with increasing flow rate, in accord with McNally, but it was convincingly demonstrated that the decrease in drag reduction was not due to polymer degradation. In the roughest pipe, there was little or no drag reduction and it was speculated that drag reduction eventually tended to vanish in fully rough flow.

The object of the present experimental investigation was to examine the physics of drag reduction in rough pipes with emphasis on the flow régimes associated with incipient and with asymptotic maximum drag reduction. For the first objective, polymers and pipe roughnesses were chosen to obtain the onset of drag reduction in each of the flow régimes—hydraulically smooth, transition, fully rough—classically associated with turbulent flow through rough pipes. For the second objective, several very high molecular weight polymers were used to induce the maximum possible drag reduction in each rough pipe and the onset of roughness under these conditions revealed the maximum viscous sublayer thickness attained during drag reduction.

2. Experimental

The test pipes used, listed in table 1 (*a*), were all of approximately 0·34 in. (0·86 cm) inside diameter. The smooth pipe S 1 was of seamless stainless steel with developing and test sections respectively 100 and 65 diameters long. Each of the three rough pipes was 60 diameters long and consisted of two equal sections of which the leading section was used to develop the flow coming in from the smooth pipe upstream while pressure differential measurements were made across the trailing section. Pipe sections were coupled by a bored out 'tee' fitting arrangement

which provided good alignment and reliable static pressure measurements. The rough pipe sections were made by cementing waterproof abrasive paper inside $\frac{1}{2}$ in. O.D. $\times$ $\frac{3}{8}$ in. I.D. lucite tubes as follows. A sheet of the proper grade paper was conditioned by rolling to successively smaller radii to prevent subsequent cracking of the abrasive matrix. From such a sheet a strip was cut to a width precisely matched to the inside diameter of the lucite casing. Epoxy cement was sparingly applied to the backing of the paper and to the inside of the lucite tube. The paper strip was then rolled loosely lengthwise over a $\frac{5}{16}$ in. O.D. stainless-steel rod, which helped guide the paper, and eased into the casing in which process the casing effectively zippered the seam. With the proper width strip the tendency of the paper to uncurl resulted in an insert with very nearly circular cross-section and a barely noticeable seam. The inside diameters of the rough pipes were ascertained three ways; first from direct micrometer measurements, second from calculations based on the measured inside diameter of each lucite casing and the thickness of the paper used and the third from laminar flow pressure drop measurements relative to the smooth pipe. For all rough pipes, the three methods agreed within 0·003 in.; values from the third method were used in all calculations and are reported in table 1. Two measures of relative roughness are given in table 1, nominal values, R/k_g, based directly on the grit size of the abrasive paper used and equivalent sand roughness values, R/k, derived (via Nikuradse 1933) from friction factors obtained with distilled water in the present experiments. The differences between k_g and k are believed to be due mainly to the orientation and geometry of the silicon carbide 'sand' particles. These particles, oriented normal to the paper surface, were found to be needle or cone shaped with aspect ratios about 1·5 and a fairly regular base diameter approximately equal to the nominal grit size. Following conventional practice, equivalent sand roughness values are used throughout this paper to characterize the rough pipes.

The five polymers used in this investigation are noted in table 1 (*b*). Of these, polyethyleneoxides N 10, N 750 and W 301 were used to study the onset of and the effect of polymeric parameters on drag reduction while the highest molecular weight polyethyleneoxide, FRA, and the pure polyacrylamide, E 117, were employed primarily to attain the asymptotic, maximum, drag reduction. All polymers were characterized by experimental intrinsic viscosity measurements from which weight average molecular weights and r.m.s. radii of gyration were obtained via light scattering data (Shin 1965; Lee 1966) for similar polymers. Polymer solutions in distilled water were prepared in a 55 gallon tank by dilution from concentrated master batches, each solution being stirred gently for 3–4 h before being run. The polymer concentrations studied are indicated in the final column of table 1 (*b*), values were determined directly from tank samples by an interferometric technique that was accurate to within $\pm(1\,\% + 2$ p.p.m.). The temperature was maintained at $25{\cdot}0 \pm 0{\cdot}5$ °C throughout.

The experiments were performed with a simple, single pass, system in which the flow was always routed through both smooth and rough test pipes in series to ensure identical flow conditions for future comparison. Gravity drainage, with flow rates regulated and measured at the downstream exit, provided

Reynolds numbers from 200 to 10,000 while a calibrated positive displacement pump was used to obtain Reynolds numbers from 8000 to 150,000. For Reynolds numbers less than 8000, the smooth pipe was 'triggered', by slightly closing a normally wide-open ball valve at its entrance, to enhance fully-developed turbulent flow. Pressure differentials between wall taps in the test pipes were

(*a*) Rough pipe characterization

Test pipe designation	I.D. in.	Grit size	R/k_g nom	R/k esr
S 1	0·333	—	—	Smooth
R 1	0·342	220	64·3	35 ± 3
R 2	0·345	150	44·2	22·8 ± 1.0
R 3	0·340	100	29·3	14·6 ± 0·5

(*b*) Polymer characterization

Designation	Species	$[\eta]$ *dl/g*	$Mw \times 10^{-6}$	*Rg* Å	Solution concentrations w.p.p.m.
N 10	PEO	0·88	0·12	390	2240, 5830
N 750	PEO	3·1	0·57	800	43·6, 98·6, 296, 939
W 301	PEO	18·5	5·5	2250	18·7, 30·6, 82·5 ± 1 (2 runs)
FRA	PEO	25	8·0	2650	110 ± 10 (3 runs)
E 117	PAM	17·5	12·5	3500	110 ± 10 (5 runs)

Notation

Nom	nominal, based on grit-size dimension k_g.
Esr	equivalent sand roughness.
PEO	Polyethyleneoxide.
PAM	Polyacrylamide.
$[\eta]$	intrinsic viscosity, decilitres/gram.
Mw	weight average molecular weight.
Rg	r.m.s. radius of gyration, Angstrom units.
w.p.p.m.	weight parts per million.

In all cases distilled water was the solvent.

TABLE 1. Experimental

measured by calibrated pressure transducers; the corresponding experimental range of wall shear stress was from 10^{-1} to 10^4 dynes/cm^2. The absolute accuracy of flow rate and pressure differential measurements was respectively ± 1 % and ± 2 %.

3. Results

3.1. *Solvent*

In the smooth pipe, experimental solvent friction factors were in good agreement with Poiseuille's law in laminar and the Prandtl–Kármán law in turbulent flow. In all rough pipes, laminar flow with solvent obeyed Poiseuille's law and turbulent flow followed well established patterns, equivalent sand roughnesses quoted in table 1 being obtained by comparison of the present friction factors with the classical results of Nikuradse (1933). In each of pipes R 2 and R 3, fully rough flow was attained over a substantial Reynolds number range and values

of R/k could be derived directly from the constant friction factors therein. For pipe R 1, in which fully rough flow was not achieved, the relative roughness was obtained by matching with Nikuradse's roughness function over the entire transitional range. Consequently the value of R/k quoted for R 1 is subject to somewhat greater uncertainty than are the R/k values for R 2 and R 3.

3.2. *Polymer solutions*

In laminar flow, all of the polymer solutions tested obeyed Poiseuille's law in all of the pipes, smooth and rough, employed.

No formal measurements were made concerning laminar to turbulent transition though it was observed that with solvent and most of the dilute polymer solutions, the transition region was approximately $2000 < Re < 2800$ in all pipes.

The onset of drag reduction is illustrated by figure 1 which has semilogarithmic Prandtl co-ordinates $1/\sqrt{f}$ *vs.* $Re\sqrt{f}$, where f and Re are the usual Fanning friction factor and Reynolds number. Figure 1 is in three parts, (*a*), (*b*), (*c*), referring respectively to pipes S 1, R 1, R 3 of table 1. In each part, data are shown for solvent (solid points) and for a single solution of each of three polyethyleneoxides; namely, 2000 p.p.m. of N 10, 100 p.p.m. of N 750 and 20 p.p.m. of W 301. In figure 1 (*a*) the polymer solutions display the characteristic behaviour associated with Toms phenomenon in smooth pipes (Virk *et al.* 1967); with all three solutions the onset of drag reduction occurs abruptly and values of $Re\sqrt{f}^*$ (the asterisk superscript will hereafter denote onset) increase inversely as polymer radius of gyration. In figures 1 (*b*) and 1 (*c*), pertaining to the rough pipes, the polymer solutions exhibit behaviour similar to that in the smooth pipe. In order of ascending $Re\sqrt{f}$, two zones of turbulent flow are identifiable; (i) a region without drag reduction in which the polymer solution friction factors are identical with solvent and (ii) a region with drag reduction wherein for any given friction velocity ($Re\sqrt{f}$) a higher bulk velocity ($1/\sqrt{f}$) is attained with the polymer solution than with solvent. As in the smooth pipe, there is sharp demarcation between regions (i) and (ii) in the rough pipes, i.e. a well-defined onset of drag reduction. From figure 1 it is seen that for a given polymer solution essentially identical values of $Re\sqrt{f}^*$ are obtained in all three pipes. Inasmuch as all pipes had the same inside diameters, this means that the onset wall shear stress, Tw^*, is the same in rough and smooth pipes. Further, and most significant, the equality between rough and smooth Tw^* holds irrespective of the rough pipe flow régime—hydraulically smooth, transition, fully rough—in which the onset of drag reduction occurs.

The effect of polymer concentration is shown by figure 2 which has a format identical to that of figure 1 except that the abcissa, $Re_s\sqrt{f}$, is based on solvent viscosity to permit comparisons directly in terms of wall shear stress. Data for four concentrations, 40, 100, 300, 1000 w.p.p.m., of a single polymer, N 750, are shown in figure 2, parts (*a*), (*b*), (*c*), which refer respectively to pipes, S 1, R 1, R 3. In each pipe, the onset of drag reduction is seen to occur approximately independently of polymer concentration, the variation in $Re_s\sqrt{f}^*$ being several orders of magnitude less than the range of concentrations. Further, for the given polymer, $Re_s\sqrt{f}^*$ values of 1150 ± 100 are observed in all pipes, indicating that the onset wall shear stress is independent of roughness at all polymer concentrations.

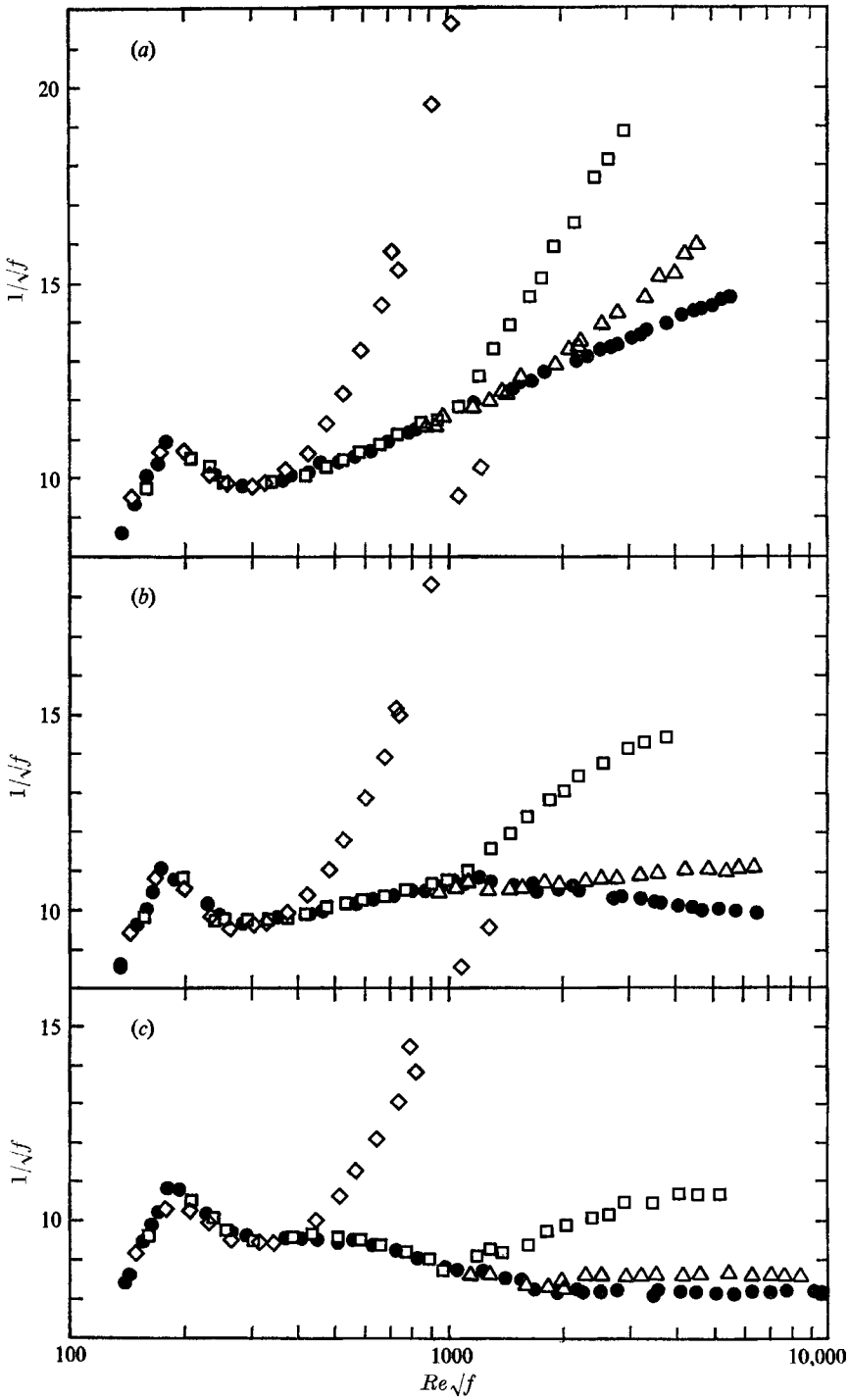

FIGURE 1. The onset of drag reduction in rough pipes. (*a*) Smooth, (*b*) $R/k = 35$, (*c*) $R/k = 14{\cdot}6$.

Symbol	Polymer	*c*, w.p.p.m.
◇	W 301	18·7
□	N 750	296
△	N 10	2240
●	Solvent	—

Onset wall shear stresses for all of the present experiments are listed in table 2 along with other pertinent results referred to in later sections.

Some features concerning the extent of drag reduction induced in the region, $Re_s\sqrt{f} > Re_s\sqrt{f}^*$, of the Toms phenomenon can also be discerned from figure 2.

Pipe		S1	R1	R2	R3	
Equivalent sand roughness R/k		Smooth	35	22·8	14·6	
			(*a*) Polymeric régime			
Polymer						Estimated error
N10	Tw^* dynes/cm^2	265	230		245	± 50
	k^{+*}		21		51	—
	k^+_{es}		55		70	± 10
N750	Tw^* dynes/cm^2	72	72		70	± 10
	k^{+*}		12		27	—
	k^+_{es}		> 40		50	± 5
W301	Tw^* dynes/cm^2	7·1	7·0		7·2	± 1·5
	k^{+*}		3·7		8·8	—
	k^+_{es}		> 16		> 40	—
			(*b*) Viscous sublayer thickness			
Solvent	$y^+_{v,n}$		4·5	5	5	± 1
Maximum drag reduction	$y^+_{v,m}$		12	12	13	± 2
Ratio	$[y^+_{v,m}/y^+_{v,n}]$		2·6	2·4	2·5	± 0·2

Notes:

* Indicates value at the onset of drag reduction.

es Denotes upper limit of effectively smooth régime.

TABLE 2. Summary of results

In the smooth pipe, figure 2(*a*), data for given solutions describe approximately straight lines on the co-ordinates employed, with slopes increasing progressively with polymer concentration. In the rough pipes, figures 2(*b*), (*c*), the data are qualitatively similar to those in the smooth pipe, in that drag reduction generally increases with increasing polymer concentration and friction velocity. However, for corresponding concentrations, individual values of $1/\sqrt{f}$ as well as the average slopes in the rough pipes are lower than in smooth and the rough pipe data affect a concave downward curvature that appears to become more pronounced as roughness is increased and as concentration is decreased. The drag reduction obtained with the very lowest concentration solutions tends to become constant at the highest friction velocities; e.g. in figure 2(*c*), 100 p.p.m. N750 in pipe R3 has $1/\sqrt{f} \sim 9{\cdot}3$ in the region $3000 < Re_s\sqrt{f} < 6000$ compared with a solvent $1/\sqrt{f}$ of 8·2 for $Re_s\sqrt{f} > 3000$.

It has previously been noted (Virk *et al.* 1967) that the maximum drag reduction possible in smooth pipes is limited by a unique asymptote which is independent of polymeric parameters; more recently, but prior to the present work, maximum drag reduction data from several sources have been correlated

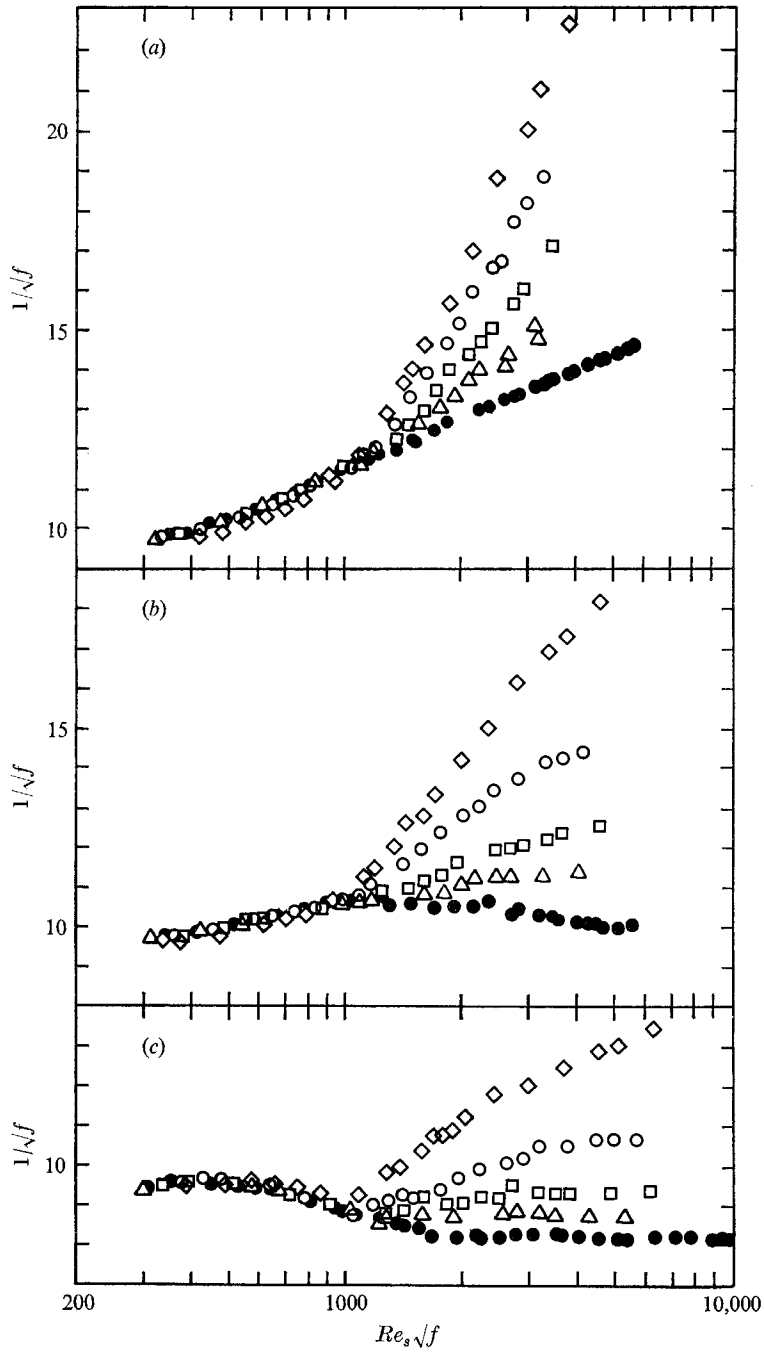

FIGURE 2. The effect of polymer concentration on rough pipe drag reduction. (*a*) Smooth, (*b*) $R/k = 35$, (*c*) $R/k = 14{\cdot}6$.

Symbol	Polymer	*c*, w.p.p.m.
◇	N 750	939
○	N 750	296
□	N 750	98·6
△	N 750	43·6
●	Solvent	—

(Virk, Mickley & Smith 1970). Rough pipe drag reduction under such asymptotic conditions is shown in figure 3, also with semilogarithmic co-ordinates $1/\sqrt{f}$ *vs.* $Re\sqrt{f}$. The solid lines on figure 3 represent Poiseuille's law, the Prandtl–Kármán law and the above-mentioned correlation of the maximum drag reduction asymptote given, respectively, by equations (1), (2) and (3) to come. The data shown in figure 3 are for solvent and two polymer solutions, 100 p.p.m. each of polyethyleneoxide FRA and polyacrylamide E 117, in the smooth pipe S 1 (solid

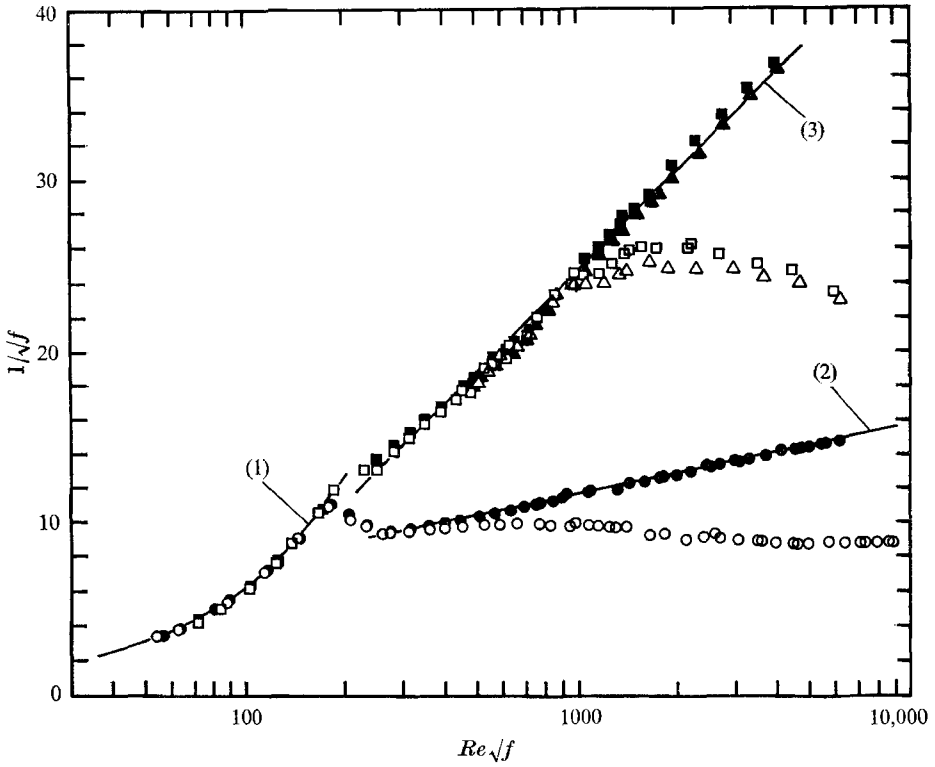

FIGURE 3. Maximum, asymptotic, drag reduction. Solid lines correspond to indicated equations in text.

Symbol R/k		Polymer	c, w.p.p.m.
Smooth	22·8		
▲	△	FRA	110
■	□	E 117	110
●	○	Solvent	—

points) and a rough pipe, R 2 (hollow points). In the smooth pipe both polymer solutions behave almost identically over the entire experimental range of $Re\sqrt{f}$ and yield friction factors which can be seen to agree well with Poiseuille's law for $Re\sqrt{f} < 180$ and with the recent correlation of the maximum drag reduction asymptote for $Re\sqrt{f} > 250$. In the rough pipe also the two polymer solutions are seen to display near identical behaviour over the entire range of $Re\sqrt{f}$. Considering only the turbulent flow régime, $Re\sqrt{f} > 200$, this indicates that in rough pipes too the drag reduction ultimately becomes independent of polymeric parameters.

Further, for each polymer solution, friction factors in the rough pipe are identical with those in the smooth pipe for $Re\sqrt{f} < 1000$. At $Re\sqrt{f} \sim 1000$ the rough pipe data peel off from the smooth data in the direction of increased friction, show a shallow maximum in $1/\sqrt{f}$ at $Re\sqrt{f} \sim 2000$ following which values of $1/\sqrt{f}$ decrease slowly up to the experimental limit of $Re\sqrt{f} \sim 6000$. Behaviour similar to the above was also observed in pipe R 1 with 100 p.p.m. solutions of polymers W 301, FRA and E 117 and in pipe R 3 with 100 p.p.m. each of FRA and E 117. To distinguish between roughness effects and polymer degradation effects, both of which result in increased friction, two experimental tests were performed at the highest flow rates with the roughest pipe. First, with the system operating in the normal once-through mode, polymer solution samples collected from the run

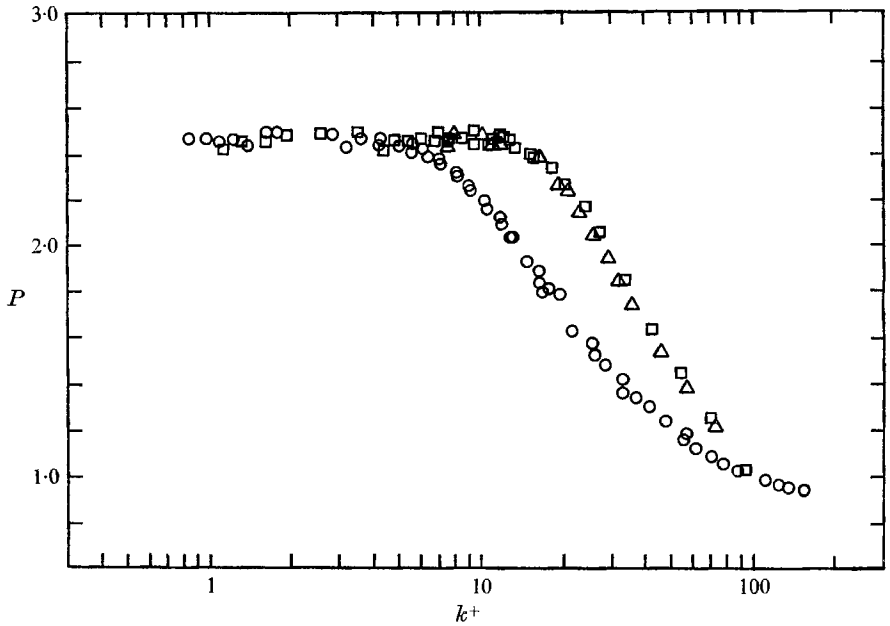

FIGURE 4. The onset of roughness during maximum drag reduction. Data of figure 3.

Symbol	Polymer	c, w.p.p.m.
△	FRA	110
□	E 117	110
○	Solvent	—

tank, from upstream of the smooth pipe and from the rough pipe exit were analysed by low shear viscometry. In all cases, all samples had practically identical relative viscosities indicating negligible degradation in one pass through the flow system. Secondly, the flow system was set up to recirculate and pressure differentials across both smooth and rough pipes were monitored with time; no change could be observed for an estimated 5 to 10 passes through the system. Both tests indicate that the features of figure 3 are not caused by polymer degradation. In which case the behaviour observed, which is strikingly analogous to that well-established for turbulent Newtonian flow through rough pipes, may

be interpreted in similar terms. Thus, under asymptotic conditions of maximum drag reduction, rough pipe R 2 appears hydraulically smooth for $Re\sqrt{f} < 1000$ while the region $1000 < Re\sqrt{f} < 6000$ has the characteristics of a transition from smooth to fully rough flow; unfortunately, the present data do not extend far enough to ascertain whether a fully rough régime exists. By way of comparison, the Newtonian flow régimes in pipe R 2, as indicated by the distilled water data also shown in figure 3, are: hydraulically smooth $Re\sqrt{f} < 300$, transition $300 < Re\sqrt{f} < 4000$ and fully rough $Re\sqrt{f} > 4000$.

The present experiments permit the end of the hydraulically smooth régime—or the onset of roughness—to be established directly by a method illustrated in figure 4. All of the data presented in figure 3 have been replotted in figure 4 on a different set of semilogarithmic co-ordinates. The abcissa is non-dimensional roughness height $k^+ = ku_\tau/\nu$ as obtained from $Re\sqrt{f}$ via the relative roughness of pipe R 2. The ordinate, P, is the ratio of the pressure differential measured in the smooth test section to that measured in the rough test section at the same flow rate. The virtue of this ordinate is that inasmuch as the same solution always flowed through both smooth and rough pipes at precisely the same flow rate, and since the geometry was fixed, the ratio of test section pressure drops depends only on the flow régime prevailing within the rough pipe. Thus throughout the hydraulically smooth régime the present ordinate stays constant and a departure from this constant value marks the onset of roughness. On figure 4 it can be seen that the onset of roughness occurs at $k^+ \sim 5$ for distilled water and at $k^+ \sim 12$ for the two polymer solutions. Note also that because of the logarithmic abscissa of figure 4, the ratio of polymer solution to distilled water k^+ at the onset of roughness is directly available from the horizontal separation between the respective sets of data at ordinates close to the constant smooth value, say $2{\cdot}2 < P < 2{\cdot}4$. All onset of roughness results are listed in table 2 (*b*).

4. Discussion

4.1. *The onset of drag reduction*

Figures 1 and 2 showed that, for a given polymer-solvent system, onset occurred at a well-defined wall shear stress Tw^* which was essentially independent of polymer concentration, pipe relative roughness and rough pipe flow régime. These assertions are substantiated by the Tw^* and k^{+*} entries in table 2 (*a*). The equality, within experimental error, between rough and smooth Tw^* values is evident. Values of the corresponding non-dimensional roughness height at onset, k^{+*}, range from 4 to 50 indicating that the onsets observed occurred over essentially the entire range of rough pipe flow from hydraulically smooth, $k^+ < 5$, to fully rough, $k^+ > 50$, with the equality between rough and smooth Tw^* unaffected thereby.

Previous work (Virk *et al.* 1967) has shown that the onset wall shear stress is related to the radius of gyration of the polymer in dilute solution. For a homologous series of polymers in a given solvent the semi-empirical relationship is of the form $Tw^* \propto Rg^{-2}$ with proportionality constant characteristic of the polymer-solvent system. A comparison of the present with previous onset data for the

polyethyleneoxide-water system is presented in figure 5 on doubly logarithmic co-ordinates of Tw^* *vs.* Rg. It can be seen that the present data (hollow points) agree well with the previous (solid points) and the entire collection is approximately described by the straight line of slope -2 drawn on the figure.

At present, comparison with the results of other investigators is limited to two rather qualitative cases, illustrated to some extent by figure 7. McNally (1968) reports friction factor data for 2 to 40 p.p.m. aqueous solutions of a

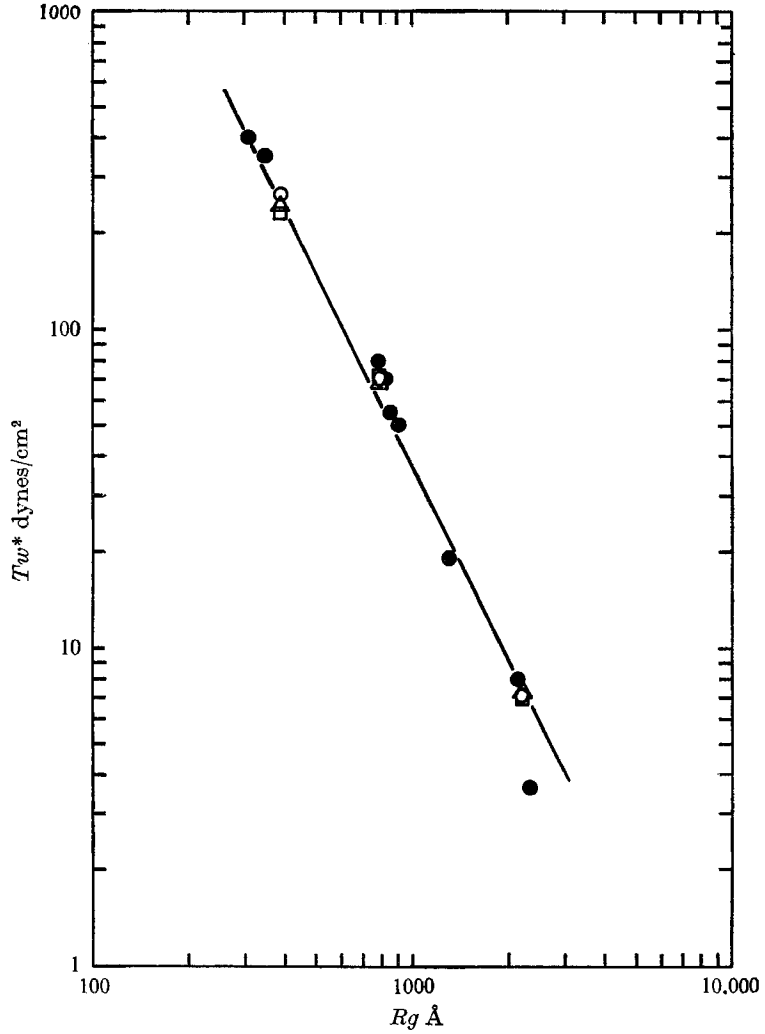

FIGURE 5. Onset correlation for polyethyleneoxide-water system.

Symbol	R/k	Pipe I.D., cm	Source
△	14·6	0·86 ± 0·01	This work
□	35		
○	Smooth		
●	Smooth	0·292, 0·945 3·21	Previous work

polyethyleneoxide, molecular weight $\sim 3{\cdot}5 \times 10^6$, flowing through 2·00 cm and 3·76 cm I.D. smooth pipes and a sand-roughened pipe of approximately 2·0 cm I.D. with $R/k \sim 3{\cdot}5$. Unfortunately, all of his data commence in regions of substantial drag reduction and the associated onset points can only be ascertained by back-extrapolation over, typically, a half decade of wall shear stress. The value of Tw^* so obtained by McNally in the 2 cm rough pipe, in which the onset of drag reduction occurs at $k^{+*} \sim 70$ during the fully rough régime, is substantially the same as in the 2 cm smooth pipe. This is in accord with the present findings. The data of Spangler (1969) also indicate approximate equality between rough and smooth onset wall shear stresses for one polymer solution in one smooth and two rough pipes in which latter onsets occurred at $k^{+*} \sim 6$ and 8.

Physically, the onset of drag reduction implies incipient polymer-turbulence interaction. The rough pipe results indicate that onset is the same whether a viscous sublayer exists (hydraulically smooth flow) or is entirely absent (fully rough flow). Whence the region wherein the polymer-turbulence interaction responsible for drag reduction starts must lie outside the viscous sublayer, $y^+ > 5$. Previous work has indicated that, for small drag reduction, conditions in the outer region of the pipe are substantially the same as Newtonian except for a uniform increase in mean velocity, or 'effective slip', that occurs some place closer to the wall than the inner edge, say $y^+ \sim 50$, of the outer flow. Taken together, the foregoing isolate the region $5 < y^+ < 50$ as the one of primary importance in the initial stages of drag reduction; this corresponds to the so-called 'buffer-layer' wherein most of the turbulent energy production and dissipation at a radial cross section are known (Laufer 1954) to take place in Newtonian turbulent flow.

4.2. *Drag reduction in the polymeric régime*

The polymeric régime is the region of flow, following onset, in which drag reduction depends upon polymeric parameters—chemical species, molecular weight, concentration. A description of this régime in smooth pipes having been presented elsewhere (Virk 1971), the attempt here is primarily to relate the respective drag reductions obtained in rough and in smooth pipes with the same polymer solution. In seeking such a relationship the observed equality of smooth and rough pipe onset shear stresses for a given polymer suggests that smooth and rough pipe drag reduction be compared at equal shear stress or friction velocity. At a given friction velocity, an appropriate measure of drag reduction is the fractional increase in mean velocity or 'slip' relative to solvent, S_F, where by definition, $S_F = (\sqrt{(f_s/f_p)} - 1)_{Re_s\sqrt{f}}$; subscripts s and p refer, respectively, to solvent and polymer solution. All of the present polymeric régime results are shown plotted as S_F *vs.* $Re_s\sqrt{f}$ in figure 6 which has three sections, (*a*), (*b*), (*c*), referring respectively to polymers W 301, N 750, N 10, in order of decreasing molecular weight. Within each section, data from pipes S 1, R 1 and R 3 are distinguished by different symbols while solution concentrations are differentiated by shading. The semi-logarithmic co-ordinates were chosen because they yield straight lines for smooth pipe data and it may be verified that such lines for all solutions of a given polymer diverge from the onset point, $(Re_s\sqrt{f}, S_F) = (Re_s\sqrt{f^*}, 0)$, with slopes

increasing approximately as the square root of concentration. The essential and remarkably simple result revealed by figure 6 is that, under certain conditions, the fractional slip in rough pipes can be *identically* the same as in smooth. As a typical example, consider the data for 300 w.p.p.m. of N 750 in figure 6 (*b*). For this polymer solution it is seen that at any given $Re_s\sqrt{f}$ the fractional slip obtained in pipe R 1, $R/k = 35$, is essentially the same as that in the smooth pipe S 1 for $1100 < Re_s\sqrt{f} < 5000$ from onset to the experimental limit. In pipe R 3, $R/k = 14.6$,

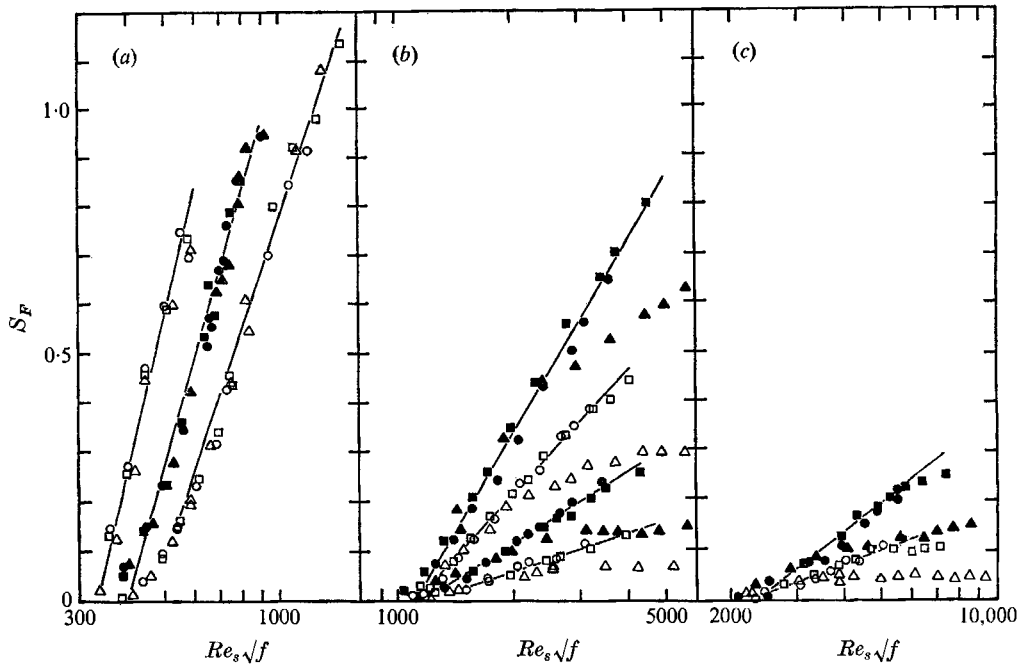

FIGURE 6. Fractional slip in rough and smooth pipes. The three sections refer to: (*a*) Polymer W 301, concentrations 18·7, 30·6, 82·5 w.p.p.m. (*b*) Polymer N 750, concentrations 43·6, 98·6, 296, 939 w.p.p.m. (*c*) Polymer N 10, concentrations 2240, 5830 w.p.p.m. Within each section the lowest concentration is represented by hollow data points, the next highest by solid points and so on alternately.

Symbol	Pipe R/k
△ ▲	14·6
□ ■	35
○ ●	Smooth

the fractional slip is essentially the same as smooth from onset to $Re\sqrt{f} \sim 2000$ at which point the R 3 data begin to diverge from smooth in the direction of lower fractional slip. It is particularly noteworthy that in the substantial $Re_s\sqrt{f}$ ranges over which the fractional slip in the respective rough pipes is the same as smooth in figure 6 (*b*), the corresponding friction factors in the rough pipes are markedly higher than smooth in figure 2. This indicates that the observations noted reflect a rough pipe phenomenon and are not due to operation of the rough pipes in the hydraulically smooth régime wherein all results must necessarily be identical with smooth. Perusal of the whole of figure 6 (*b*) will demonstrate that the

behaviour described for the 300 w.p.p.m. solution applies to all other concentrations of polymer N 750 as well. It is further interesting that the R 3 data all diverge from smooth at $Re_s\sqrt{f} \sim 2000$ independently of polymer concentration though their behaviour in the region $Re_s\sqrt{f} > 2000$ is concentration dependent; e.g. for the 40 w.p.p.m. solution the fractional slip tends to a constant value with increasing $Re_s\sqrt{f}$ whereas for the 1000 w.p.p.m. solution the fractional slip, while less than smooth, continues to increase strongly with increasing $Re_s\sqrt{f}$. The features noted in figure 6(*b*) are equally apparent in figures 6(*a*) and (*c*) except that the different polymer molecular weights alter the magnitudes involved. In figure 6(*a*), polymer W 301, onset occurs at $Re_s\sqrt{f^*} \sim 400$ and the fractional slip in each of pipes R 1 and R 3 is much the same as in the smooth pipe S 1 over the entire experimental range. In figure 6(*c*), polymer N 10, onset is at $Re_s\sqrt{f^*} \sim 2200$, the data for pipe R 1 depart from smooth at $Re_s\sqrt{f} \sim 5500$ whereas those for pipe R 3 depart at $Re_s\sqrt{f} \sim 3000$.

In the general case of rough pipe drag reduction by dilute polymer solutions there thus exists a flow régime, hereafter termed 'effectively smooth', in which the fractional slip relative to solvent is the same as would be obtained in a smooth pipe of the same internal diameter operating at the same friction velocity. The term 'effectively' smooth is intended to imply an equality between rough and smooth fractional slip irrespective of the corresponding friction factors as distinct from the conventional 'hydraulically' smooth case wherein rough and smooth friction factor relationships, and hence fractional slip are identical. While our experimental results do not cover the hydraulically smooth case to any great extent, the few such data in figure 6(*a*), pipe R 1, suggests that a hydraulically smooth region, if any occurs, would be the initial portion of an effectively smooth régime as defined above. Figure 6 also showed that, for a given polymer, the friction velocity at which the rough pipe fractional slip data depart from smooth is independent of polymer concentration but does depend upon relative roughness; corresponding values of non-dimensional roughness, termed k_{es}^+, for all polymers in both pipes are shown in table 2. In all cases the upper limit of the effectively smooth régime is $k_{es}^+ \sim 50$.

The existence of an effectively smooth régime cannot as yet be confirmed from external sources but the few data available in the literature (McNally 1968, Spangler 1969) lend some support to the present observations. McNally's data, shown in figure 7(*a*) as S_F *vs.* $Re_s\sqrt{f}$, indicate a rough pipe fractional slip always less than the corresponding smooth slip over the range $1000 < Re_s\sqrt{f} < 5000$. Inasmuch as the lowest experimental $Re_s\sqrt{f} \sim 1000$ corresponds to $k^+ \sim 100$, which exceeds the upper limit $k_{es}^+ \sim 50$ of the effectively smooth régime, McNally's results are in qualitative agreement with ours. A more direct test is provided by the data of Spangler (1969), shown replotted on our co-ordinates in figure 7(*b*), for a single polymer solution in one smooth and two threaded-wall type of rough pipes of about equal inside diameters. In figure 7(*b*) the fractional slip in the pipe with $R/k = 47$ is approximately the same as smooth over a substantial range from onset, $Re_s\sqrt{f^*} \sim 800$, to $Re_s\sqrt{f} \sim 5000$ while data from the $R/k = 36$ pipe are the same as smooth over a shorter range $800 < Re_s\sqrt{f} < 2000$. These results are evidently in accord with ours though the departure from smooth in

the two rough pipes of figure 7(*b*) occurs at $k^+ \sim 40$ and 20 which values are somewhat lower than obtained in our experiments.

At friction velocities exceeding the upper limit of the effectively smooth régime the fractional slip in the rough pipes is always less than that in the corresponding smooth pipe. In this region, $k^+ > k_{es}^+$, the present experiments,

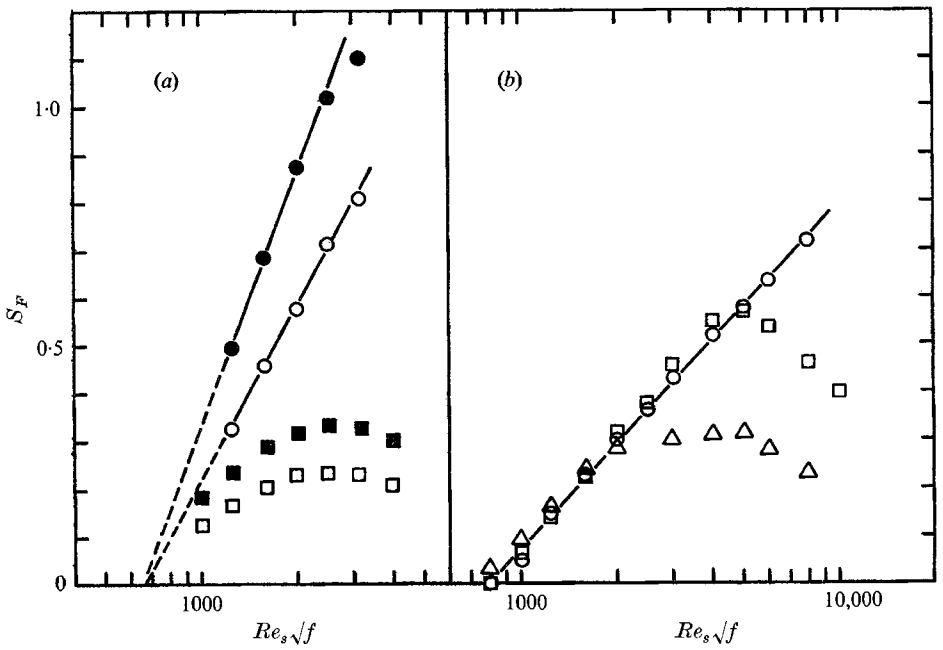

FIGURE 7. Data of other investigators in fractional slip co-ordinates. (*a*) McNally (1968). 20 and 40 w.p.p.m. of a polyethyleneoxide, $Mw \sim 3{\cdot}5 \times 10^6$, in water. (*b*) Spangler (1969). 31 w.p.p.m. of an acrylic acid-acrylamide copolymer, $Mw \sim 5 \times 10^6$, in water.

Part	Symbol	Pipe R/k	Pipe I.D., cm	c, w.p.p.m.
(*a*)	□	3·5	2·0	20
	○	Smooth		20
	■	3·5		40
	●	Smooth		40
(*b*)	△	36	1·9	31
	□	47		31
	○	Smooth		31

figure 6, indicate a general tendency for the fractional slip to level off with increasing k^+ (i.e. $Re_s\sqrt{f}$) while the results of other investigators (McNally 1968; White 1969; Spangler 1969) show that it is also possible for the fractional slip to decrease with increasing k^+, presumably to an eventual level of little or no drag reduction. However, no cohesive patterns can be discerned and the nature of rough pipe drag reduction in the polymeric régime as k^+ is increased indefinitely remains to be investigated.

4.3. *Maximum drag reduction*

In smooth pipes, the drag reduction obtained in the polymeric régime is ultimately limited by an asymptote which is independent of polymeric parameters (Virk *et al.* 1967) and the present experiments, figure 3, indicate an analogous asymptote in rough pipes as well. The analogy is more fully illustrated by figure 8

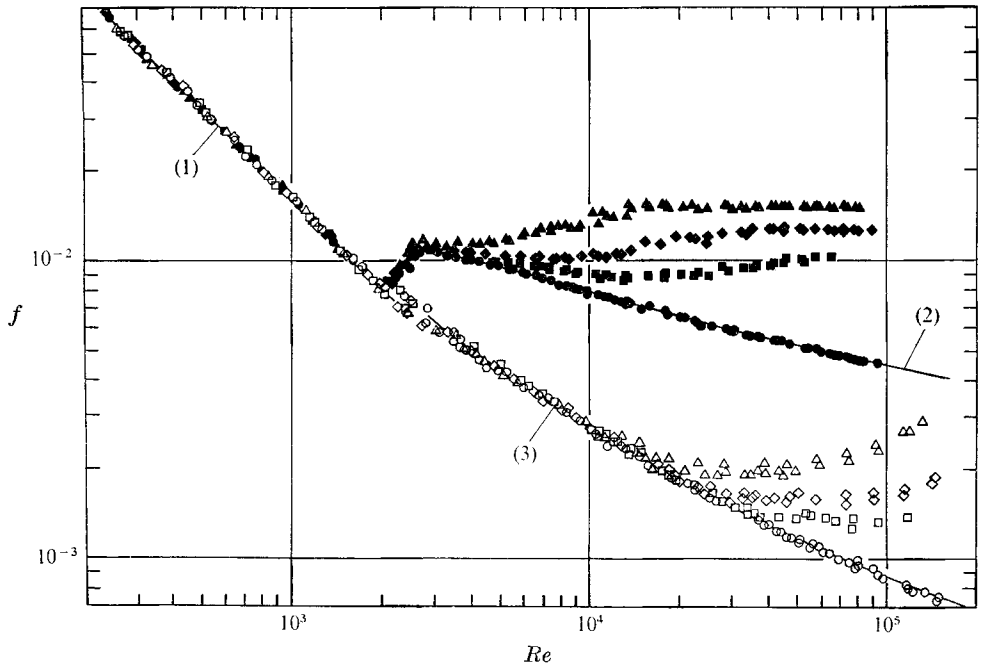

FIGURE 8. Friction factor plot for maximum asymptotic drag reduction in rough pipes. Solid points refer to solvent, hollow points to polymer solutions yielding maximum drag reduction.

Symbol	R/k
△ ▲	14·6
◇ ◆	22·8
□ ■	35
○ ●	Smooth

wherein all of the present maximum drag reduction data are displayed on conventional, doubly logarithmic, friction factor *versus* Reynolds number coordinates. In figure 8, the one smooth and three rough pipes involved are distinguished by separate symbols, the solid points refer to solvent data and the hollow points denote maximum drag reduction data; for clarity, the individual polymer solutions used to attain maximum drag reduction are not differentiated, having been noted earlier. The three solid lines on figure 8 represent, respectively, Poiseuille's law for Newtonian laminar flow

$$1/\sqrt{f} = Re\sqrt{f}/16; \tag{1}$$

the Prandtl–Kármán law for turbulent Newtonian flow in smooth pipes:

$$1/\sqrt{f} = 4{\cdot}0\log_{10}(Re\sqrt{f}) - 0{\cdot}4; \tag{2}$$

and the author's recent correlation (Virk, Mickley & Smith 1970) for turbulent flow at asymptotic maximum drag reduction in smooth pipes:

$$1/\sqrt{f} = 19{\cdot}0\log_{10}(Re\sqrt{f}) - 32.4. \tag{3}$$

For $Re < 2000$, it can be seen that *all* data obey Poiseuille's law (1). This Newtonian behaviour in laminar flow stems from and illustrates well the very dilute nature of the polymer solutions involved. In turbulent flow, $Re > 3000$, the respective sets of solvent and polymer solution data show striking similarities with respect to the effect of pipe roughness. In the smooth pipe, the solvent data obey the Prandtl–Kármán law (2) for $3000 < Re < 90{,}000$ while the polymer solutions follow the maximum drag reduction asymptote (3) for $3000 < Re < 150{,}000$. In the three rough pipes, R 3, R 2, R 1, the solvent data are initially the same as, but then diverge from smooth at Reynolds numbers, respectively about 2500, 3000, 5000, which increase with increasing R/k. Likewise, at maximum drag reduction, data from pipes R 3, R 2, R 1 are identical with smooth up to respectively, $Re \sim 12{,}000$, 20,000, 30,000 whence they depart from smooth in the direction of increased friction. Finally, following their respective departures from smooth, the rough pipe friction factors exhibit shallow minima in both Newtonian and maximum drag reduction cases; but whereas the Newtonian set proceed to a régime of constant friction factors at the highest Reynolds numbers, the maximum drag reduction data terminate before any such trend can be detected.

The similarities between Newtonian and maximum drag reduction flows in rough pipes lead naturally to a general description of the latter by means of the roughness function, β, where

$$\beta = \sqrt{(2/f)} + 3/2\chi - (1/\chi)\ln(R/k). \tag{4}$$

Although the roughness function was originally defined (Nikuradse 1933) for Newtonian flows, it is clear that (4) and the arguments leading to it will also apply at asymptotic drag reduction since the maximum drag reduction asymptote (3) has a semilogarithmic form identical to the Prandtl–Kármán law (2). The mixing length constant χ will, of course, differ according to the coefficients of (2) and (3), appropriate values being $\chi_n \sim 0{\cdot}40$ for Newtonian and $\chi_m \sim 0{\cdot}085$ for maximum drag reduction. In the Newtonian case, β is well known to be a universal function of the non-dimensional roughness height, k^+, and this relationship is classically interpreted in terms of the universal mean flow structure in the pipe (Nikuradse 1933). Roughness functions derived from the present experiments are shown in figure 9, a semilogarithmic plot of β *vs.* k^+ with symbols identical to those of figure 8. It can be seen that the solvent data (solid points) are in fair agreement with Nikuradse's results (solid line) over the entire range $3 < k^+ < 300$. The broken line on figure 9 represents the hydraulically smooth relation

$$\beta = 11{\cdot}7\ln k^+ - 16{\cdot}1, \tag{5}$$

expected under asymptotic conditions by direct inference from the corresponding friction factor relation (3). The maximum drag reduction data (hollow points) from all rough pipes lie parallel to and are approximately given by (5) for $k^+ < 12$ (the mean curve through the data for $3 < k^+ < 12$ is somewhat better described by changing the constant $-16{\cdot}1$ to -17). At $k^+ \sim 12$, the onset of roughness, the data begin to depart from (5) and it is interesting to note that, despite considerable scatter, roughness functions from all three pipes appear to be universal in the rough régime $k^+ > 12$ on figure 9 in contrast to the distinct differences between their respective friction factors in the corresponding portions of figure 8.

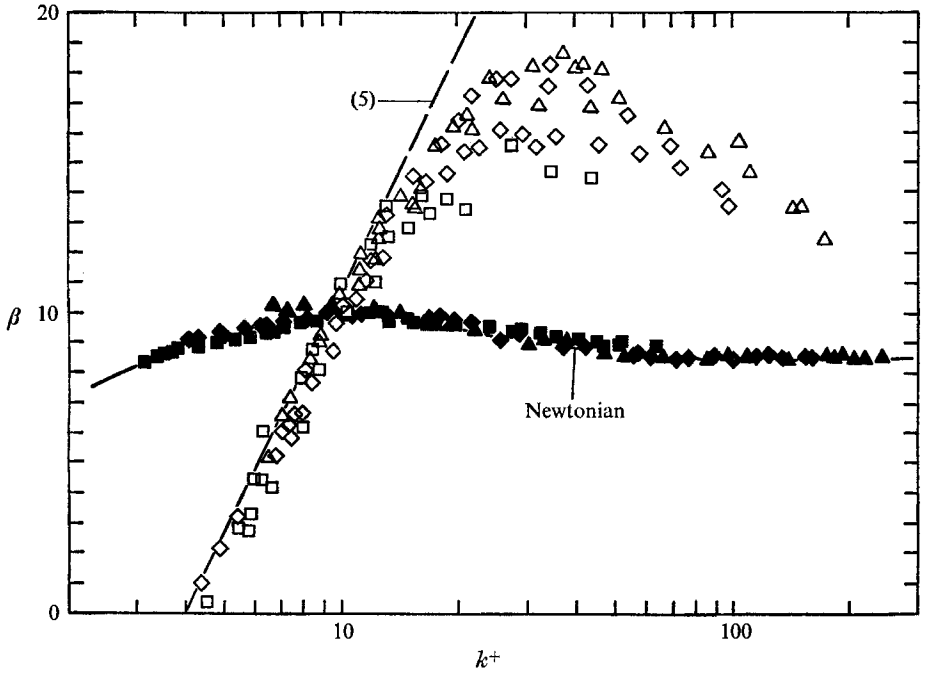

FIGURE 9. Roughness function for maximum drag reduction. Data, legend same as figure 8. Solid line marked 'Newtonian' is from Nikuradse (1933); broken line represents equation (5) in text.

The region $12 < k^+ < 150$ up to the upper experimental limit seems to be a transition from smooth to fully rough flow but the question of a fully rough régime under asymptotic conditions remains to be examined.

By the usual reasoning, the non-dimensional sand roughness height k^+ at the onset of roughness can be considered synonymous with the non-dimensional thickness of the viscous sublayer y_v^+ in the preceding hydraulically smooth régime. Viscous sublayer thicknesses thus obtained from the present experiments by the sensitive method of figure 4 are quoted in table 2 under the headings $y_{v,n}^+$ for Newtonian, $y_{v,m}^+$ for maximum drag reduction and $[y_{v,m}^+/y_{v,n}^+]$ for their ratio. With solvent, $y_{v,n}^+ = 5 \pm 1$, in reasonable agreement with the usual Newtonian value of 5; at maximum drag reduction, all pipes yield $y_{v,m}^+ = 12 \pm 2$, the ratio of asymptotic to Newtonian thicknesses being $2{\cdot}5 \pm 0{\cdot}2$. Now, the viscous sublayer 'thickness' is somewhat arbitrary because the ratio of turbulent to

viscous transport, i.e. eddy to kinematic viscosity ϵ/ν, increases continuously from the wall outward in this region and thus the usually accepted Newtonian value $y^+_{v,n} \sim 5$ is better associated with its corresponding $\epsilon/\nu \sim 0{\cdot}1$ (numerical value from Laufer 1954). Therefore, the ratio $[y^+_{v,m}/y^+_{v,n}]$ is probably best interpreted physically as a radial separation between points of equal ϵ/ν within the respective viscous sublayers; for example, if $\epsilon/\nu \sim 0{\cdot}1$ at $y^+ \sim 5$ in the Newtonian case, then $\epsilon/\nu \sim 0{\cdot}1$ at $y^+ \sim 5 \times 2{\cdot}5 \sim 12$ under conditions of maximum drag reduction and similar factors of 2·5 would separate all points of equal ϵ/ν for $\epsilon/\nu < 0{\cdot}1$. This basic result can be extended to comparisons at equal y^+ since very near a smooth wall the eddy viscosity tends to a cubic (or higher) power law in distance from the wall, i.e.

$$\epsilon/\nu = \alpha(y^+)^3; \quad y^+ \to 0, \tag{6}$$

where α is a proportionality constant. If the power law (6) is assumed to hold to the outer edge of the viscous sublayer and this outer edge taken as a location of equal ϵ/ν in each case the ratio of proportionality constants is

$$[\alpha_m/\alpha_n] = [y^+_{v,m}/y^+_{v,n}]^{-3} \sim 0{\cdot}06.$$

Thus, at a given y^+ near the wall, the eddy viscosity during maximum drag reduction is attenuated to about 0·06 times the Newtonian value.

The inference concerning eddy viscosity can be tested by mass (or heat) transfer at high Schmidt number ($Sc \to \infty$) which is controlled by turbulent transport in the viscous sublayer. Under these conditions the dimensionless wall mass transfer coefficient M^+ depends simply upon the eddy viscosity relation (6) and the ratio of maximum drag reduction to Newtonian mass transfer should be the reciprocal of the viscous sublayer thickness ratio, i.e. $[M^+_m/M^+_n] = [y^+_{v,m}/y^+_{v,n}]^{-1}$, assuming that the Schmidt number in the dilute polymer solutions used to induce maximum drag reduction is the same as Newtonian. Preliminary mass transfer measurement in our laboratory under conditions of maximum drag reduction in a smooth pipe yield a direct experimental value $[M^+_m/M^+_n] \sim 0{\cdot}5$ for $Sc \sim 10^3$ which gives a viscous sublayer thickness ratio $[y^+_{v,m}/y^+_{v,n}] \sim 2$. The approximate agreement between values of $[y^+_{v,m}/y^+_{v,n}]$ obtained from separate mass transfer and rough pipe measurements is interesting.

With regard to turbulent flow structure, eddy viscosity can be decomposed into appropriate turbulent length and velocity scales, the former being the so-called 'mixing' length while the latter is most directly associated with the radial intensity of turbulence, v'. Of these, the friction factor relationships (2) and (3) directly indicate that the non-dimensional mixing length during maximum drag reduction is reduced relative to Newtonian by the ratio $[\chi_m/\chi_n] \sim 0{\cdot}2$. Whence, since the observed sublayer thickening corresponds to an eddy viscosity attenuation by a factor $\sim 0{\cdot}06$, the radial turbulence intensity in the viscous sublayer must be reduced by a factor $0{\cdot}06/0{\cdot}2 \sim 0{\cdot}3$ relative to Newtonian. This is, of course, a most tentative conclusion and whilst no data are available for sublayer turbulence structure during maximum drag reduction it is noteworthy that the results of Seyer & Metzner (1969), do indicate markedly lower than Newtonian values of radial intensity at all locations from the pipe centreline to as close to the wall as $y^+ \sim 30$.

To the best of our knowledge, no data have previously been reported for maximum drag reduction in rough pipes, precluding comparison with the present.

5. Conclusions

From the present experiments it is possible to identify five régimes in the flow of dilute polymer solutions through smooth and rough pipes:

Laminar flow

In this régime Poiseuille's law was obeyed by all dilute polymer solutions in smooth and rough pipes.

Laminar-to-turbulent transition

This régime was not formally studied; casual observation indicated that in both smooth and rough pipes the polymer solutions behaved much as the solvent.

Turbulent flow without drag reduction

In this régime the polymer solutions obeyed identically the same friction factor relation as the solvent, i.e. the Prandtl–Kármán law in the smooth pipe and Nikuradse's equivalent sand roughness modification thereof in the rough pipes.

Turbulent flow with drag reduction dependent upon polymeric parameters—the polymeric régime

The onset of drag reduction. In both smooth and rough pipes, this occurred at a well-defined wall shear stress Tw^* which was independent of polymer concentration but varied inversely as the square of the polymer radius of gyration Rg in dilute solution. For a given polymer, the onset wall shear stress in a rough pipe was the same as in the smooth pipe, irrespective of the flow régime prevailing in the rough pipe at onset. In terms of non-dimensional roughness, this latter was varied from $k^{+*} \sim 4$ lying in the hydraulically smooth régime to $k^{+*} \sim 50$ which corresponds to fully rough flow and throughout this range identical values of Tw^* were obtained in rough and smooth pipes for each of three polymers.

The 'effectively smooth' régime. Following onset, the drag reduction induced by a given polymer solution is a complex, as yet not fully defined, function of flow and polymeric parameters and of pipe roughness. However, the drag reduction in rough pipes was found to be simply related to that in smooth over a range $k^{+*} < k^+ < k_{es}^+$, termed the effectively smooth régime; throughout this régime the fractional slip, S_F, induced by a given polymer solution at a given friction velocity in a rough pipe was the same as the fractional slip obtained under identical circumstances in a smooth pipe of the same inside diameter. The upper limit of the effectively smooth régime was independent of polymer concentration and molecular weight and pipe relative roughness—a single value, $k_{es}^+ \sim 50$ approximately described all of the present data.

For $k^+ > k_{es}^+$ the fractional slip observed in the rough pipes was always less than that corresponding to smooth but no general trends could be discerned regarding the nature of drag reduction as k^+ is increased indefinitely.

Turbulent flow with drag reduction independent of polymeric parameters—the maximum drag reduction asymptote

In both smooth and rough pipes the maximum possible drag reduction was limited by an asymptote which was independent of polymeric parameters. In the smooth pipe this maximum drag reduction asymptote was described by a (previously derived) friction factor relation (3) of a semilogarithmic form similar to the Prandtl–Kármán law (2). Under conditions of maximum drag reduction, the effect of pipe roughness was analogous to that well known for Newtonian turbulent flow and could be described by a universal asymptotic roughness function β which was solely dependent on non-dimensional roughness k^+. For $k^+ < 12$, the hydraulically smooth régime, friction factors in all rough pipes precisely obeyed the smooth pipe maximum drag reduction asymptote (3). The onset of roughness occurred at $k^+ \sim 12$; this implies that during drag reduction the viscous sublayer can, at maximum, be thickened to approximately $2\frac{1}{2}$ times Newtonian. For $k^+ > 12$, the asymptotic rough régime, the present experiments indicated a transitional region $12 < k^+ < 150$ wherein the asymptotic roughness function increased from $12 < k^+ < 30$, exhibited a shallow maximum at $30 < k^+ < 50$ and then decreased with increasing k^+ up to the experimental limit $k^+ \sim 150$. This latter was not high enough to give any indication regarding asymptotic behaviour as k^+ increases without limit.

The author is indebted to Professor H. S. Mickley and K. A. Smith of the Chemical Engineering Department for their interest in this work and to the Sloan Basic Research Fund and the ONR for financial assistance.

REFERENCES

ELATA, C., LEHRER, J. & KAHANOVITZ, J. 1966 *Israel J. Technol.* **4**, 87.

LAUFER, J. 1954 *N.A.C.A. Rep.* 1174.

LEE, T. S. 1966 Sc.D. Thesis, M.I.T., Cambridge, Mass.

LINDGREN, E. R. & HOOT, T. G. 1968 *ASME J. Appl. Mech.* **35**, 417.

MCNALLY, W. A. 1968 Ph.D. Thesis, Univ. of Rhode Island.

NIKURADSE, J. 1933 *N.A.C.A. Tech. Mem.* 1292 (translated).

ROOT, R. L. 1966 *Method for Decreasing Friction Loss in a Well Fracturing Process.* U.S. Patent no. 3, 254, 719.

SAVINS, J. G. 1964 *Soc. Petrol. Engng J.* **4**, 203.

SEYER, F. A. & METZNER, A. B. 1969 *A.I.Ch.E. J.* **15**, 426.

SHIN, H. 1965 Sc.D. Thesis, M.I.T., Cambridge, Mass.

SPANGLER, J. G. 1969 In *Viscous Drag Reduction.* (Ed. C. S. Wells.) Plenum.

TOMS, B. A. 1948 *Proc. Ist Int. Congress on Rheology*, vol. 2, p. 135. North-Holland.

VIRK, P. S. 1971 *J. Fluid Mech.* **45**, 417.

VIRK, P. S., MERRILL, E. W., MICKLEY, H. S., SMITH, K. A. & MOLLO-CHRISTENSEN, E. L. 1967 *J. Fluid Mech.* **30**, 305.

VIRK, P. S., MICKLEY, H. S. & SMITH, K. A. 1970 *ASME J. Appl. Mech.* **37**, 488.

WHITE, A. 1969 In *Viscous Drag Reduction.* (Ed. C. S. Wells.) Plenum.